# Piercing of Aluminum Beverage Cans

**Brian A. Coon**
Graduate Research Assistant, University of Nebraska-Lincoln

**Phanidhar Anugonda**
Graduate Research Assistant, University of Nebraska-Lincoln

**John D. Reid**
Associate Professor, University of Nebraska-Lincoln
Mechanical Engineering Department
N104 WSEC (0656)
Lincoln, NE 68588
(402) 472-3084
jreid@unl.edu

*Keywords:*
Aluminum Beverage Cans, Impact Simulation, Nonlinear Finite Element Analysis

## ABSTRACT

An LS-DYNA finite element model was developed to analyze the structural behavior of an aluminum beverage can subjected to a piercing load applied to the sidewall of the can. Physical testing was performed to help verify the simulation accuracy. The piercing was intended to simulate the damage to a can that might occur during the manufacturing process. Impacts of 5 m/s and 10 m/s were performed with both blunt (flat) and sharp (45 tip) steel rods. It was found that separated elements with tied nodal constraints more accurately represent the behavior of the can subjected to a piercing load than merged element nodes. It was also found that the more crushing a can undergoes before piercing occurs, the more energy the can material absorbs. However, there is an upper limit to the crushing based on the speed and shape of the impactor.

## INTRODUCTION

The purpose of this research project was to investigate the piercing of empty aluminum cans using LS-DYNA finite element analysis software and compare the results with physical testing of the same event. LS-DYNA is a transient, nonlinear finite element analysis program that uses explicit time integration (Hallquist, 1997). Final results of this project should yield a highly validated aluminum can model for piercing that may be useful for the design of future cans.

## BACKGROUND

Previous studies completed by Robert Dick (Dick, 1994) of the Aluminum Company of America (Alcoa), Scott Magner (Magner, 1997), and Robert Bielenberg (Bielenberg, 1998) have used finite element analysis to simulate the buckling of undeformed aluminum cans, the denting of the sidewall of the can, and the buckling of a dented can, respectively. However, the piercing of the sidewall of the can had not been explored.

The initial Alcoa aluminum can model was designed to simulate the axial buckling of an undeformed aluminum can subjected to a load along the vertical axis. The aluminum material for the can was modeled as an elasto-plastic material, which allowed the stress-strain curve and strain rate dependency to be defined. The model utilized a Belytschko-Tsay shell element formulation. The contact definition for the model was specified as an automatic single surface type contact. The Alcoa model fairly accurately predicted the buckling of undeformed aluminum can sidewalls when compared with physical testing (Dick, 1994).

## FINITE ELEMENT MODELING METHODOLOGY

The simulation of the piercing of the can required several changes to the Alcoa model. The rigid ground below the bottom of the can was replaced with one along the side. The moving wall providing the buckling load was removed and replaced with a piercing rod along the side of the can opposite of the ground (see Figure 1). Since the steel rod used to impact the can was three times stiffer (Young s modulus) than the can itself and over 100 times thicker, the piercing rod was modeled as a rigid body. During physical testing, neither the plate used to support the can or the steel rod used for piercing had any measurable deformations. Thus, modeling these features as rigid is a reasonable assumption.

Figure 1. Piercing Can Model

The steel rod impacts the can at the center of the sidewall, where the Magner study indicated that maximum deformations occurred. The impact was centered across the horizontal axis of

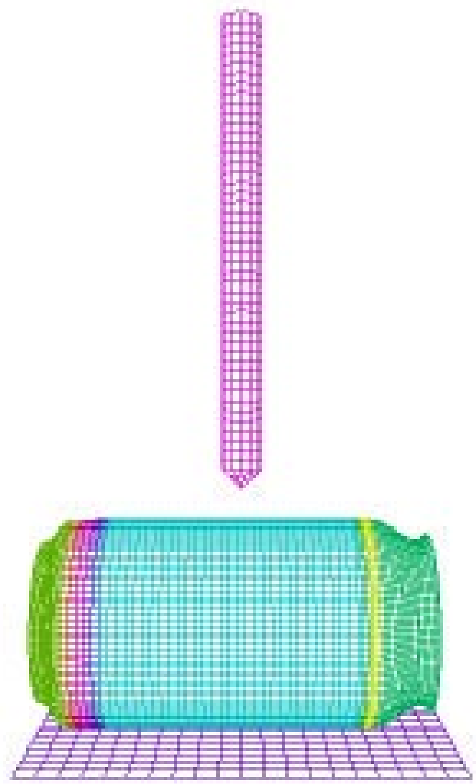

the can.

Previous can simulation studies had not specified a strain failure criterion. Thus, in order to achieve failure of the can due to piercing, a strain failure criterion of 9.4% was added to the model (ASM, 1979).

In addition to specifying a strain failure criterion, the elements of the can were modeled using tied nodes with failure, where the shell elements were separated and then tied together with nodal constraints. When the volume-weighted average of the failure value is reached for a group of constrained nodes, the nodes of the elements that exceed the failure value are released to simulate the tearing of the can. It was necessary to change the model to tied nodes with failure, as opposed to specifying a direct material failure criteria, in order to better simulate the aluminum tearing as seen in the physical testing.

When the element nodes are merged, the elements are deleted as the strain failure criterion is met. The deleting of the material causes huge gaps in the can to develop, as shown in Figure

2(a). When the elements are separated and the nodes are tied with nodal constraints, a tearing of the material occurs similar to physical testing, as shown in Figure 2(b).

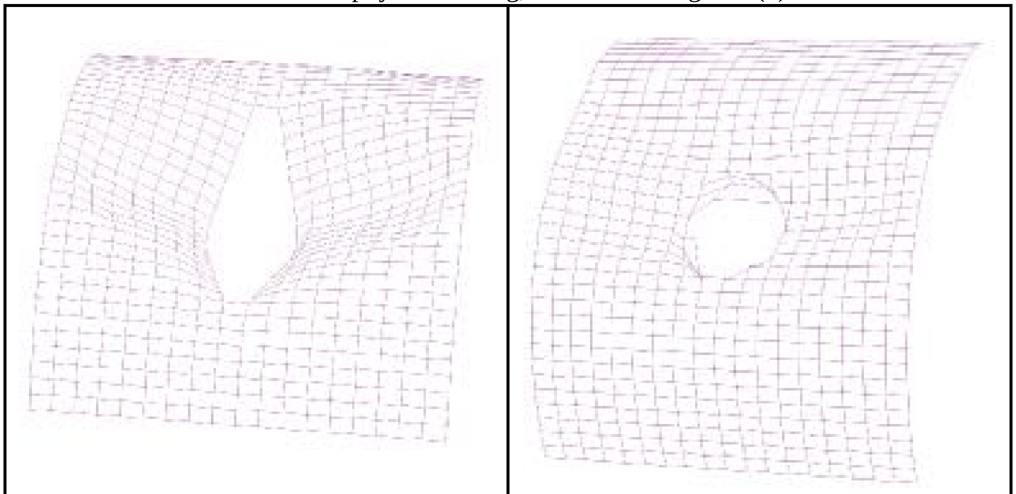

| (a) Merged Nodes | (b) Tied Nodes |
| --- | --- |

Figure 2. Effects of Tied Nodal Constraints on Failure Mode

In addition to the mode of failure, tied nodal constraints also greatly influences the load transfer and amount of energy absorbed during piercing. When tearing occurs with tied nodes, significantly higher forces and more energy absorption was observed than the model with merged nodes.

The model output was investigated in detail to check for any basic modeling problems such as incorrect input, unrealistic behaviors, and hourglass energy modes. The results showed no obvious errors and relatively little hourglassing effects.

## PHYSICAL TESTING METHODOLOGY

It was desired to impact the can at multiple velocities and be able to control the amount of energy being inputted into the system. This allowed a direct comparison of energy input versus energy absorbed by the can. In order to attain a known energy level, the mass and velocity of the steel rod were both controlled. The mass of the steel rod was 148 g, and the velocity of the steel rod was determined using basic physics.

A conduit system was built to drop the steel rod from a known height (see Figure 3). Assuming no friction existed between the wall of the conduit and the rod, the velocity of the rod was calculated using the equations of motion with constant acceleration. Starting from an initial velocity of zero, the velocity of any free-falling object subject to the Earth s gravity can be found using the equation:

$$v = \text{sqrt}\,(2\ a_g\ H) \qquad \text{[Eqn 1]}$$

Where $a_g$ is the acceleration of gravity and H is the height from which the object is dropped. For this experiment, the effects of air resistance were neglected.

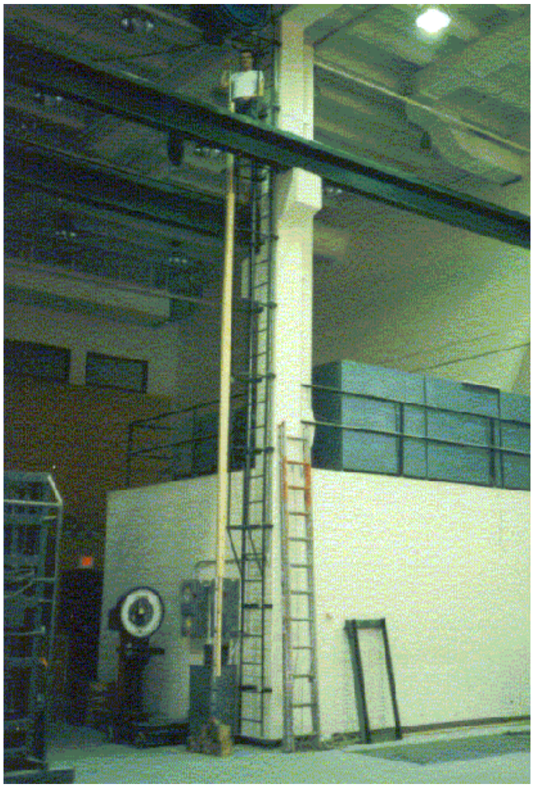

Figure 3. Testing Apparatus

Both sharp and blunt six-inch steel rods were used in physical testing. The blunt rods were machined flat on the ends while the sharp steel rods were machined with a 45 tip. The can rested on a surface of 60 ksi flat steel one-quarter inch thick. Tests were performed on empty beverage cans that had been consumed by University students.

To load the testing apparatus, a half-inch woven wire rope was used to press the steel rod up into the tube. This was done to protect the tip of the steel rod, since loading the rod from the top of the apparatus had damaged prior tips significantly. Once the rod had reached the appropriate height, a nail was inserted to hold the steel rod in place. When the nail was removed, the steel rod fell freely down the conduit impacting the can. Five tests were performed for each velocity and for each tip; a total of twenty impacts of empty cans were performed and documented with photographs and deformation measurements. Additionally, eight full cans were impacted.

## COMPARISON OF RESULTS

The deformed and undeformed geometries of the aluminum cans from the LS-DYNA simulation and physical testing are shown in Figure 4 and Figure 5. The variations of the lettering orientation are the result of the random process used to paint the Coca-Cola® logo onto the cans. In order to maximize the reproducibility of the test results, the mouth of the can was oriented upward during all impacts. This does not appear to be detrimental to the model, since the top of the can appears to have remained rigid during physical testing.

| | |
|---|---|
| 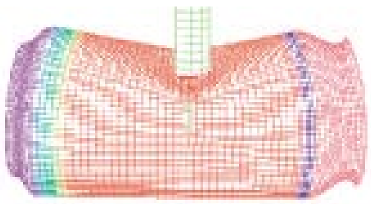 | 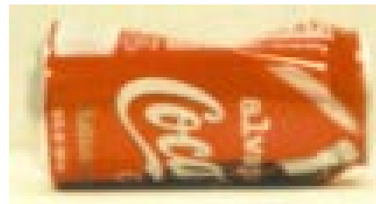 |
| (a) LS-DYNA Simulation | (b) Testing |
| 5 m/s Impact | |
| 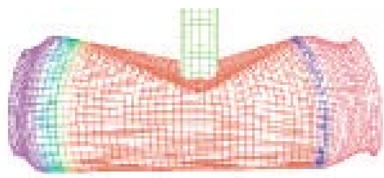 |  |
| (c) LS-DYNA Simulation | (d) Testing |
| 10 m/s Impact | |

Figure 4. Results for Sharp Rod (45° tip)

| | |
|---|---|
| 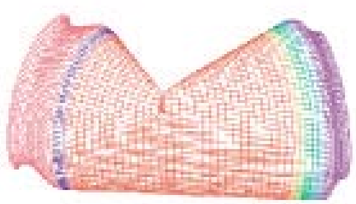 |  |
| (a) LS-DYNA Simulation | (b) Testing |
| 5 m/s Impact | |

| 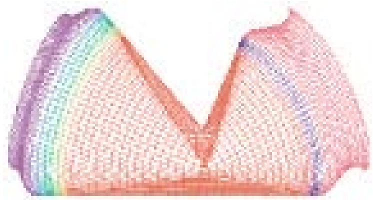 |  |
|---|---|
| (c) LS-DYNA Simulation | (d) Testing |
| 10 m/s Impact | |

Figure 5.  Results for Blunt Rod

*Sharp Steel Rod Penetration*
Results for the physical test data and simulation for the sharp steel rod were very similar in failure modes and final deformation (Figure 4).  Piercing of the can, both in the simulation and in physical testing, resulted in the tearing of the thin aluminum sidewall where penetration occurred.  After the steel rod had penetrated the first sidewall, the rod continued through the can and impacted the opposite sidewall.  This resulted in the creation of a small hole where the opposite sidewall was impacted between the sharp steel rod and the rigid wall.

*Blunt Steel Rod Penetration*
The model and the physical testing demonstrated similar deformed shapes for the blunt rod penetration (Figure 5). The denting of the can in the simulation occurred at the center of the can where physical testing saw failure occur diagonally across the can.  This failure mode was seen in all blunt steel rod impacts, even when penetration occurred in the 10-m/s physical test and finite element model.

*Energy Absorption*
The amount of energy absorbed in the impact was also examined.  Finite element modeling showed a steel rod with an impact velocity of 10 m/s with a blunt tip absorbed more energy than any of the other cases modeled.  However, there was only a 4% difference between the 5 m/s and 10 m/s blunt rod energies absorbed with a 4 times greater initial energy.  It would appear energy levels start to become asymptotic to a maximum energy level absorbed.

Differences in energy levels between the blunt and sharp tips are thought to be the result of the crushing of the can that occurs during the impact of the blunt tip rather than the piercing that was seen with sharp-tip rods.  The energies absorbed by the can are shown in Figure 6.

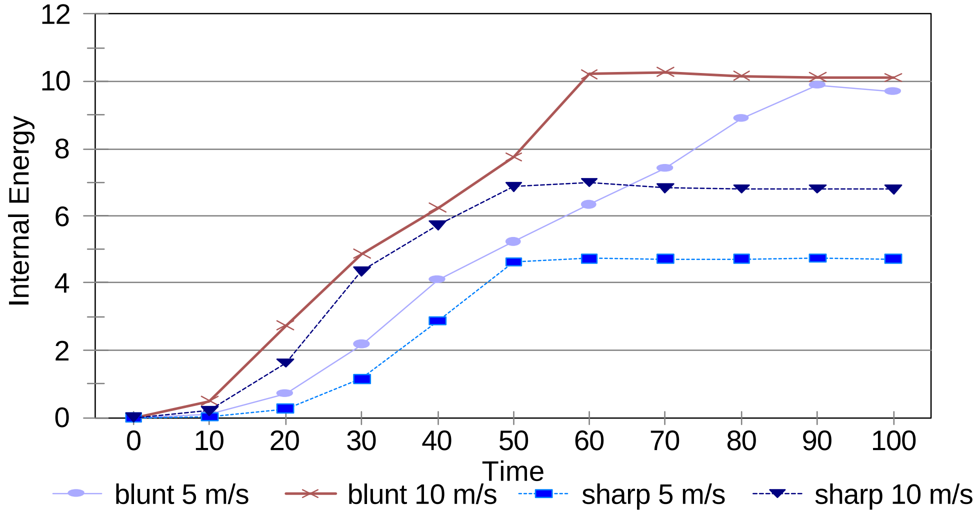


Figure 6. Energy Absorbed by Can Material

The maximum energy absorbed by the can material appears to be directly related to the amount the can is crushed for the sharp rod. As shown in Table 1, more energy is absorbed when a blunt rod impacts a can. The blunt rod caused significantly more deformation than the sharp rods, which pierced immediately into the can. Also, there appears to be a maximum amount of energy that can be absorbed by the can when impacted by the blunt rod.

*Comparison of Deformed Shapes and Failure Modes*

For both the blunt and sharp steel rods, the deformed shapes were measured and recorded from physical testing as well as from nodal output data from the LS-DYNA simulation. Deformed shapes, as well as failure modes, compared extremely well, varying less than 5% from physical testing. Failure modes were consistently similar, provided great care was taken to align the can with the impacting steel rod, assuring identical impacts between physical testing and computer simulation.

Table 1. Peak Energy Absorption of Can Material.

| | Impact Velocity | |
|---|---|---|
| | 5 m/s | 10 m/s |
| Initial Kinetic Energy of the Piercing Rod | 1850 N-mm | 7400 N-mm |
| Blunt Tip Design Internal Energy Absorbed | 1116 N-mm | 1164 N-mm |
| 45 Sharp Tip Design Internal Energy Absorbed | 536 N-mm | 789 N-mm |

## CONCLUSIONS AND RECOMMENDATIONS

The study of the piercing of aluminum cans using LS-DYNA led to several conclusions and recommendations. First, finite element simulation closely matched actual physical testing data for the piercing of aluminum cans. There was a strong correlation between both failure modes and the amount of deformation seen between physical testing and simulation.

The energy differences between tied nodes and merged nodes shows the importance of verifying the type of failure mode undergone. Significant differences in failure mode, deformations, and energy levels were observed when elements with merged nodes were separated and tied together with nodal constraints. This produced not only a more realistic failure model similar to that observed in physical testing, but also drastically increased the energy absorbed by the can.

A large portion of the variation between tied nodes and merged nodes is due to the physical reality being represented. The amount of energy absorbed by a can is more dependent on the amount of crushing that occurs, rather than the amount or speed of piercing. Lower impact velocities absorbed nearly as much energy as the higher ones due to similar amounts of deformation. Since the merged nodes model saw virtually no crushing, energy levels were significantly less than energy levels of the tied nodes.

The pierced can model adequately represents the deformed geometry and failure modes experienced in actual physical testing. However, there is an opportunity for further development and improvement. The influence of different rod sizes and piercing locations could be explored. Physical testing could be improved by incorporating various measurement techniques to capture load transfer and accelerations. Finally, testing and simulating the piercing of a fully pressurized beverage is recommended.

## ACKNOWLEDGMENTS

The authors acknowledge Bob Dick (Alcoa), Scott Magner (UNL), Bob Bielenberg (UNL) and LSTC for their support and help on this project.

## REFERENCES

ASM (1979). American Society for Metals, Metals Handbook Ninth Edition, Vol. 2, ASM, Metals Park, Ohio, 1979.

Bielenberg, R.W. (1998). Finite Element Analysis of the Buckling of Deformed Aluminum Beverage Cans Using LS-DYNA, prepared for Impact Engineering, University of Nebraska-Lincoln, December 1998.

Dick, R.E. (1994). Axial Buckling of Beverag Can Sidewalls, 2nd International LS-DYNA3D Conference, San Francisco, CA, September 20-21, 1994.

Hallquist, J.O. (1997). *LS-DYNA Keyword User s Manual*, Livermore Software Technology Corporation, Livermore, CA, June 1997.

Magner, S.H. (1997). Side Indentation of Aluminum Beverage Cans, prepared for Impact Engineering, University of Nebraska-Lincoln, December 1997.